Atmos. Chem. Phys. Discuss., doi:10.5194/acp-2015-986, 2016
Manuscript under review for journal Atmos. Chem. Phys.
Published: 5 February 2016

Atmospheric Chemistry and Physics Discussions

On the simultaneous deployment of two single particle mass spectrometers at an urban background and a road side site during SAPUSS

Manuel Dall'Osto[1,2*], David C. S. Beddows[3], Eoin J. McGillicuddy[4], Johanna K. Esser-Gietl[3,5], Roy M. Harrison[3,$] and John C. Wenger[4]

[1*]Institut de Ciències del Mar, Consejo Superior de Investigaciones Científicas (CSIC), Pg Marítim de la Barceloneta 37-49, 08003 Barcelona, Spain; Tel: 0034 644 053 801; Email: dallosto@icm.csis.es

[2]Institute of Environmental Assessment and Water Research (IDAEA) Consejo Superior de Investigaciones Científicas (CSIC) C/ Jordi Girona 18-26 08034 Barcelona, Spain

[3]National Centre for Atmospheric Science Division of Environmental Health & Risk Management School of Geography, Earth & Environmental Sciences, University of Birmingham, Edgbaston, Birmingham, B15 2TT, United Kingdom

[4]Department of Chemistry and Environmental Research Institute, University College Cork, Ireland

[$]also at: Department of Environmental Sciences/Center of Excellence in Environmental Studies, King Abdulaziz University, Jeddah, 21589, Saudi Arabia

[5] now at: Deutscher Wetterdienst, Meteorological Observatory Hohenpeißenberg, Hohenpeißenberg, Germany

Atmos. Chem. Phys. Discuss., doi:10.5194/acp-2015-986, 2016
Manuscript under review for journal Atmos. Chem. Phys.
Published: 5 February 2016

Atmospheric Chemistry and Physics Discussions

Abstract

The Aerosol Time-of-Flight Mass Spectrometer (ATOFMS) provides size resolved information on the chemical composition of single particles with high time resolution. Within SAPUSS (Solving Aerosol Problems by Using Synergistic Strategies), continuous ATOFMS measurements of ambient particles were made simultaneously at two urban locations: urban background (UB) site and road side (RS) site in the city of Barcelona (Spain) from 17th September to 18th October 2010. Two different instrumental configurations were used: ATOFMS (TSI 3800) with a converging nozzle inlet (high efficiency at about 800-2000nm) at the UB site and ATOFMS (TSI 3800-100) with an aerodynamic lens inlet (high efficiency at about 300-700nm) at the RS site. This is the first time, to our knowledge, that two ATOFMS instruments have been deployed in the same field study. The different instrument configurations had an impact on the observed particle types at the two sites. Nevertheless, ten particle types were detected at both locations, including local and regional elemental carbon (22.7-58.9% of total particles), fresh and aged sea salt (1.0-14.6%), local and regional nitrate -containing aerosols (3-11.6%), local lead-containing metallic particles (0.1-0.2%) and transported Fe-nitrate particles (0.8-2.5%). The ATOFMS at the UB also characterised four particle types: calcium-containing dust (0.9%), Saharan dust (1.3%), vanadium-containing particles (0.9%) and vegetative debris (1.7%). By contrast, the high statistical counts of fine particles detected at the RS allowed identification of eight particle types. Four of these contained amines of primary and secondary origin. Aminium salts were found related to coarse sulphate rich particle types, suggesting heterogeneous reaction mechanisms for their

Atmos. Chem. Phys. Discuss., doi:10.5194/acp-2015-986, 2016
Manuscript under review for journal Atmos. Chem. Phys.
Published: 5 February 2016

Atmospheric Chemistry and Physics Discussions

formation. The other four particle types mainly containing organic carbon were found spiking at different types of the day, showing a complex single particle mixing state relationship between organic carbon and nitrate. This ATOFMS study clearly shows that the composition of atmospheric fine particles in Barcelona, and likely other Mediterranean urban areas, is complex, with a wide range of local and regional sources combining with chemical processing to produce at least twenty-two different particle types exhibiting different temporal behaviour. The advantage of using two ATOFMS instruments is also demonstrated, with the nozzle-skimmer configuration enabling detection of coarse dust particles and the aerodynamic lens configuration allowing better identification of particles rich in organic carbon and amines.

Atmos. Chem. Phys. Discuss., doi:10.5194/acp-2015-986, 2016
Manuscript under review for journal Atmos. Chem. Phys.
Published: 5 February 2016

Atmospheric Chemistry and Physics Discussions

1

2

3 **1. Introduction**

4

5 A substantial number of studies have shown a relationship between measures of
6 particulate air pollution and a variety of adverse health indicators (WHO, 2004).
7 Formulation of cost-effective air pollution control policies depends upon a sound
8 knowledge of source contributions to ambient concentrations. Only with such
9 knowledge can realistic cost-benefit evaluations be conducted. The major sources of
10 ambient particles in most urban areas are primary emissions from road traffic and
11 other fuel combustion, secondary particles arising from condensation or chemical
12 processing, and resuspension of soils and road dusts (AQEG, 2005; Harrison et al.,
13 2012). Marine aerosol can also contribute in coastal locations and the interactions of
14 anthropogenic trace gases with natural aerosol (i.e. dust, sea salt) can also have
15 significant effects on aerosol composition (Abbatt et al., 2012).

16 Measurement of particle composition by on-line mass spectrometry has developed
17 extensively over the last two decades and is currently the fastest growing area of
18 atmospheric aerosol research (Laskin et al., 2012). The aerosol time-of-flight mass
19 spectrometer (ATOFMS) has been used in many previous field studies to determine
20 the chemical constituents of atmospheric aerosols (Pratt and Prather, 2012). It can
21 identify both refractory and non-refractory species in single particles and can provide
22 size-resolved information on particle sources and atmospheric processing at high
23 time resolution (Prather and Pratt, 2012; Laskin et al., 2012;). The ATOFMS has
24 been used in a number of recent field studies in urban areas of Europe (Dall´Osto

Atmos. Chem. Phys. Discuss., doi:10.5194/acp-2015-986, 2016
Manuscript under review for journal Atmos. Chem. Phys.
Published: 5 February 2016

and Harrison, 2012; Healey et al., 2013) to identify and characterise particles from a diverse range of anthropogenic sources including traffic, solid fuel burning, industry, soil and road dust, marine aerosol and secondary aerosol formation processes. However, it is worthy of mention that ATOFMS source apportionment capabilities are limited by the difficulties in quantification of its outputs (Reilly et al., 2000; Schoolcraft et al., 2001). However, single-particle analysis is an important analytical tool that allows us to determine how the myriad chemical constituents are distributed between individual particles (mixing state, Pratt and Prather, 2012). The ATOFMS has often reported a number of particle types, which at times are difficult to associate with a specific aerosol source (Pastor et al., 2003; Dall´Osto and Harrison 2006; 2012).

The objective of the present manuscript is to report a detailed analysis of the ATOFMS particle types detected during a field measurement campaign carried out in Barcelona, Spain, as part of the SAPUSS (Solving Aerosol Problems by Using Synergistic Strategies) project . The ATOFMS cannot provide quantitative aerosol mass loading concentrations, but its strength relies in the fact that it can monitor in real time variations in the single particle composition. In other words, small variations in the particle mixing state results in a single particle mass spectra. As a result, a number of atmospheric processes and aerosol sources can be monitored in real time. In this paper we discuss, not only information on the mass spectra, but also diurnal trends persisting over four weeks are discussed. Further information on the intensive field campaign can be found in the presenting overview paper found in this ACP special isssue (Dall´Osto et al., 2012a). Two different ATOFMS instruments were deployed during the four-week measurement period - one at a Road Side (RS) site and the other at an Urban Background (UB) site. This is the first time an ATOFMS has been deployed in Spain and, to the best of our knowledge, it is also the

Atmos. Chem. Phys. Discuss., doi:10.5194/acp-2015-986, 2016
Manuscript under review for journal Atmos. Chem. Phys.
Published: 5 February 2016

first time (worldwide) that two ATOFMS instruments have been deployed simultaneously in the same field campaign. The similarities and differences in particle types detected at both sites is described in detail and attributed to a range of local and regional sources, as well as to different chemical and physical processes.

2. Methods

2.1 Location

The SAPUSS field measurement campaign involved a large variety of instrumentation deployed simultaneously at a number of monitoring sites in Barcelona (Spain), between 17th September and 18th October 2010 (local time, UTC+2) (Dall´Osto et al., 2012). ATOFMS measurements were made at the two main SAPUSS supersites:

- Road side (RS) site was situated in a car park next to a major road (Carrer Urgell). The road, which crosses the city from South East to North West, is a street canyon composed of a two-way cycling path and a one-way four lane vehicle road. Vehicle intensity for the month of measurements was about 17,000 vehicles per day.
- Urban Background (UB) site was situated in a small park at the North Western periphery of the city centre. A main road (Avenida Diagonal, 127,000 vehicles/day) is located about 500 m away from the site.

Atmos. Chem. Phys. Discuss., doi:10.5194/acp-2015-986, 2016
Manuscript under review for journal Atmos. Chem. Phys.
Published: 5 February 2016

The two sites were about 2 km from each other (Dall'Osto et al., 2012). While the UB site was open to wind from all directions, the wind flow and turbulence at the RS site were affected by the nearby street canyons and vehicular traffic.

2.2 Instrumentation

The mass spectrometers were housed in air-conditioned trailers at both sites. Sampling was performed ca. 4 m above ground using a quarter-inch internal diameter stainless steel tube fitted with a $PM_{2.5}$ cyclone. The sample air was dried before arriving at the instruments. The two ATOFMS instruments used in this study had different configurations. The instrument deployed at the RS site was an ATOFMS TSI model 3800-100, in which particles are sampled through an orifice and accelerated through an aerodynamic lens to the sizing region of the instrument (Su et al. 2004). By contrast, the instrument at the UB site was an ATOFMS TSI Model 3800 that utilized a converging nozzle inlet (Gard et al. 1997). Both instruments provide the aerodynamic diameter of particles sizes between about 100 nm and 3 µm by calculating their time of flight between two orthogonally positioned continuous wave lasers (λ = 532 nm). However, the transmission efficiencies of the two instruments are quite different. While the aerodynamic lens affords a much higher transmission efficiency for particles with diameters less than about 1 µm, its performance for larger particles is not as good as the converging nozzle inlet. Following the sampling and sizing, particles are transferred to the mass spectrometry region where a pulsed laser (λ = 266 nm, about 1 mJ $pulse^{-1}$) desorbs and ionizes material within the particle in the centre of the ion source of a bipolar reflectron ToF-MS. Thus, positive and negative ion mass spectra of a single particle are obtained. Overall, during the SAPUSS field study the ATOFMS was operating for 68% and

Atmos. Chem. Phys. Discuss., doi:10.5194/acp-2015-986, 2016
Manuscript under review for journal Atmos. Chem. Phys.
Published: 5 February 2016

97% of the time at the UB and at the RS site, respectively. It is also worth noting that an inter comparison of the two instruments was attempted at the same site, but this could not be completed due to complex logistical and technical factors.

The ATOFMS datasets were imported individually into YAADA (Yet Another ATOFMS Data Analyzer) and single-particle mass spectra were grouped with adaptive resonance theory neural network, ART-2a (Song et al. 1999). The parameters used for ART-2a in this study were: learning rate 0.05, vigilance factor 0.85, and 20 iterations. Further details of the parameters can be found elsewhere (Dall'Osto and Harrison 2006; Rebortier and Prather 2007). An ART-2a area matrix (AM) of a particle cluster represents the average intensity for each m/z for all particles within a group. An ART-2a AM therefore reflects the typical mass spectra of the particles within a group.

3. Results

3.1 ATOFMS particle detection efficiency

Overall, 890,873 particle mass spectra were apportioned at the RS and 221,139 at the UB. This large difference in detected particle numbers is likely a result of the combined effects of the location and detection efficiencies of both instruments. As shown in Figure 1, the number and size distribution of the particles detected by the two mass spectrometers is quite different and reflects their expected performance characteristics (Gard et. al., 1997; Su et al., 2004). The instrument with the aerodynamic lens detected considerably more particles below 1 µm, while particles larger than ca. 1.9 µm were only detected with the converging nozzle inlet. By

Atmos. Chem. Phys. Discuss., doi:10.5194/acp-2015-986, 2016
Manuscript under review for journal Atmos. Chem. Phys.
Published: 5 February 2016

running ART-2a, more than 300 clusters were found initially in both UB and RS datasets. Many were merged if they presented similar temporal trends, size distributions and mass spectra (Dall´Osto and Harrison, 2006). By merging similar clusters, the total number of particle types describing the whole dataset was reduced to 18 and 14 at the RS and UB sites, respectively. Despite the different inlet configurations and sampling locations, the majority of the particles detected at both sites could be described by 10 common ATOFMS particle types, listed in Table 1. A number of other particle types were found only at one of the monitoring sites (8 at the RS site and 4 at the UB site), likely due to the different urban environments, as well as the different detection efficiency of the two instruments (Table 1).

3.2 ATOFMS particle types observed at both sites

3.2.1 Elemental Carbon (EC)

Two main EC particle types, representing together more than 50% of detected particles (58.9% at the UB, 53.8% at the RS), were identified at both sites. For reasons outlined below, they are named EC_Aged_R (Regional) and EC_Aged_L (Local). Both EC particle types presented a fine aerosol size distribution mode at both sites (about 300-500 nm, see Fig. SI1). Fig. 2a shows the positive mass spectrum of particle type EC_Aged_R. It is dominated by EC peaks at m/z 12 $[C]^+$, 36 $[C_3]^+$, 48 $[C_4]^+$ and 60 $[C_5]^+$. Cluster EC_Aged_L (see Fig. 2b) also shows a similar EC positive mass spectrum pattern, although a strong signal at m/z 39 dominates the positive mass spectrum. This peak is often associated with potassium $[K]^+$, although

Atmos. Chem. Phys. Discuss., doi:10.5194/acp-2015-986, 2016
Manuscript under review for journal Atmos. Chem. Phys.
Published: 5 February 2016

Atmospheric Chemistry and Physics Discussions

there may also be a contribution from the organic ion $[C_3H_3]^+$ (Dall´Osto et al., 2009). The EC signals present in the positive mass spectra, and the near-total absence of peaks in the negative mass spectra suggests these EC particles are not freshly emitted. Indeed, Giorio et al. (2012) reported for a regional background site that strong EC peaks in the negative ion mass spectrum are more indicative of fresh emissions while strong EC peaks in the positive mode represent aged elemental carbon. This is consistent with observations which indicate that particle composition affects the ionization and fragmentation pattern of EC (Reinard and Johnson, 2008). The two EC-rich particle types were mainly detected in stagnant air masses. As shown in Fig. SI 1a, an enhancement of these particle types was observed during sulfate-rich air masses (7-10 October 2010) and nitrate-rich stagnant regional air masses (13-17 October 2010), as described in Dall´Osto et al., (2012). The diurnal profiles of these two aged EC particle types (Fig. 3a) can also help to classify their origin. Whilst EC_Aged_R shows little diurnal variation, particle type EC_Aged_L shows a gradual increase during the day, peaks in the afternoon (15:00) and drops to a minimum during night time. The absence of sharp morning peaks indicates that these EC particle types are not associated with primary emission from local traffic. Similarly, the absence of a sharp evening peak also excludes the association with biomass burning, which is not expected at this time of the year and is generally not important in Barcelona (Dall´Osto et al., 2012). Whilst the flat diurnal trend of EC_Aged_R is typical of regional aerosol, particle type EC_Aged_L suggests a local influence, or an enhancement during the warmer part of the day. This assignment is also supported by the observed correlation of the EC types with some secondary inorganic particle types associated with local and regional aerosol sources, described in the next section. Similar conclusions were recently reported by Decesari et al.

Atmos. Chem. Phys. Discuss., doi:10.5194/acp-2015-986, 2016
Manuscript under review for journal Atmos. Chem. Phys.
Published: 5 February 2016

(2014), where most of the aged EC particles detected with the ATOFMS were related to aged anthropogenic aerosols accumulating in the lower layers of the Po Valley (Italy) overnight.

3.2.2 Secondary nitrate and sulfate

The application of the ART-2a neural network algorithm to the ATOFMS data apportioned two main distinct nitrate particle types, already previously reported (Dall´Osto et al., 2009; Harrison et al., 2012; Decesari et al.,2014). The first ("Loc-NIT" Local-Nitrate; 4.2-7.3% particles by number) appears to be locally produced in urban locations during night time, whilst the second ("Long Range Transport" nitrate, LRT-NIT 4.2-7.3% of particles by number) is regionally transported within the Iberian Peninsula and the rest of Europe. Briefly, particle type Loc-NIT is characteristic of nitrate aerosol in small particles (D_a at about 300–500 nm; Fig. SI2). The average mass spectrum (Fig. 2c) shows a peak at m/z 39 that can be due to potassium, although previous studies (Dall'Osto et al., 2009) suggested that an organic contribution may be also present depending on the m/z 39/41 ratio. The ATOFMS nitrate particle type appears to be associated with local formation processes and occurred in the main at times outside of the long-range transport episode (Fig SI 2b). By contrast, a second nitrate particle type (Long Range Transport nitrate, LRT-NIT) is regionally transported. The average mass spectrum (Fig. 2d) shows that nitrate (m/z -62) is internally mixed with sulfate (m/z -97), ammonium (m/z 18) and both elemental (m/z 36, 48, 60) and organic carbon (m/z 37, 39, 43). As explained in Decesari et al. (2014) these aerosols likely originate from the night-time condensation of nitric acid on EC-containing primary particles (e.g. Shiraiwa et al., 2007). The LRT-NIT particle type is volatile, and partially evaporates during the day

Atmos. Chem. Phys. Discuss., doi:10.5194/acp-2015-986, 2016
Manuscript under review for journal Atmos. Chem. Phys.
Published: 5 February 2016

leaving a core of about 300 nm mainly composed also of sulfate, elemental and organic carbon (Dall'Osto et al., 2009). Indeed, this can be seen in the LRT-SUL (Long Range Transport - Sulfate) particle type, whose average mass spectrum for this (Fig. 2e) shows peaks due to nitrate (m/z -62), sulfate (m/z -97), elemental carbon (m/z -36, 48, 60) and organic carbon (m/z -39, 43). The LRT-SUL and LRT-NIT diurnal trends are clearly anti-correlated (Fig. 3b), with LRT-SUL concentrations peaking in the afternoon hours. Such behaviour is attributed to the effect of the diel cycle of nitric acid and ammonia condensation/evaporation on the same particle type: during night-time this regional particle type is seen with nitrate, which evaporates during daytime leaving a smaller aerosol core composed of EC and sulfate (Decesari et al., 2014). However, this study shows a novel aspect not found in the London local-regional nitrate study (Dall´Osto et al., 2009) or in the Po Valley (Decesari et al., 2014). During the period 12-14 October, under rainy conditions and with air masses arriving from Europe (Dall´Osto et al., 2012) the transport of LRT-SUL was detected without the nitrate component (LRT-NIT, Fig. S1b). This could be due to a different source of LRT-SUL not linked with LRT-NIT, and previously unobserved.

3.2.3 Potassium Organo-Nitrogen (K-CN) particles

The K-CN particle type was a minor one, representing only 1.3-2,4% of the total particles analyzed. Fig. 2f shows the average mass spectrum, which features a strong peak at m/z 39 $[K]^+$in the positive mode, as well as peaks at m/z 113 $[K_2Cl]^+$ and m/z -35 $[Cl]^-$ suggesting a biomass burning source (Pastor et al., 2003; Dall´Osto and Harrison, 2006). K-rich particles similar to K-CN have previously been

Atmos. Chem. Phys. Discuss., doi:10.5194/acp-2015-986, 2016
Manuscript under review for journal Atmos. Chem. Phys.
Published: 5 February 2016

attributed to biomass burning (Silva et al., 1999; Guazzotti et al., 2003) and were found to correlate with gas-phase measurements of acetonitrile, a good biomass-burning tracer. The negative ion mass spectrum shows strong peaks at m/z - 26 $[CN]^-$ and m/z -42 $[CNO]^-$, indicating that the potassium and chloride is internally mixed with organo-nitrogen species. The size distribution, centred at about 350 nm (Fig. SI 2) also points to a combustion source. Overall, this particle type represented only about 2% of the total particles sampled (Table 1) and its temporal variation is presented in Fig. SI 2d. Its diurnal trend (Fig. 3) tracks the anthropogenic activities of the city of Barcelona, suggesting general minor urban combustion processes. It should be noted that biogenic plant debris also has a similar single particle mass spectrum, with strong signals at m/z 39, - 26 and -42 (Silva et al., 2000). However, vegetative dust is usually internally mixed with sodium and phosphate, and presents aerodynamic diameters above 1 µm (see section 3.3).

3.2.4 Fresh and aged sea salt particles

Two sea salt particle types (fresh and aged) were detected at both sites, accounting for 9.4% and 18.3% of the total particles sampled at RS and UB, respectively (Table 1). The average mass spectrum (Fig. 2g) for the particle type assigned to fresh sea salt (labelled NaCl) shows peaks typical of sodium chloride clusters ($[Na]^+$ (m/z 23), $[K]^+$ (m/z 39), $[Na_2]^+$ (m/z 46), $[Na_2Cl]^+$ (m/z 81 and 83), $[NaCl_2]^-$ (m/z 93, 95 and 97), whilst aged sea salt (NaCl-NIT, Fig. 2h) also exhibited nitrate peaks (m/z –46 and m/z –62) reflecting the reaction between NaCl and HNO_3 and the replacement of chloride by nitrate (Gard et al., 1998). Both particle types had mean size distributions

Atmos. Chem. Phys. Discuss., doi:10.5194/acp-2015-986, 2016
Manuscript under review for journal Atmos. Chem. Phys.
Published: 5 February 2016

above 1 µm (Fig. SI 2 c). NaCl was mainly detected during air masses that had travelled over Mediterranean regions (7-10 and 11-13 October), as shown in Fig SI 2e. Interestingly, the diurnal variation of the two NaCl particle types is quite different (Fig. 3) .Whilst aged sea salt (NaCl-NIT) does not show a clear trend, the fresh sea salt (NaCl) shows an enhancement in the afternoon, associated with the sea breeze, peaking at 15:00 (Dall´Osto et al., 2012).

3.2.5 Iron and Lead containing particles

Two common ATOFMS particle types have average mass spectra that were dominated by metals. The first was rich in iron (type Fe, 1.4% of the total particles) and has a spectrum (Fig. 2i) characterised by a strong signal at m/z 56 and weaker features at m/z 73 (iron oxide, $[FeOH]^+$) and m/z 54 (isotope $[^{54}Fe]$). The negative spectra spectrum has strong features at m/z -46 and -62, indicating that the iron is internally mixed with nitrate. During SAPUSS, the Fe particle type was found to correlate (R^2=0.75) with LRT-NIT, which is associated with long range transport of pollutants. The small mode of the Fe particle type (Fig SI 2) reflects the fact that only fine particles were likely to travel long distances relative to the coarser ones which were lost during transport. This is in line with previous ATOFMS field studies showing the transport of iron-containing particles internally mixed with nitrate from continental Europe (Harrison et al., 2012). The flat diurnal profile for the Fe particle type (Fig. 3) also suggests a regional origin.

The average mass spectrum of the second metal-rich particle type is shown in Fig. 2j. This particle type is labelled Pb since lead is one of the largest contributors in the

Atmos. Chem. Phys. Discuss., doi:10.5194/acp-2015-986, 2016
Manuscript under review for journal Atmos. Chem. Phys.
Published: 5 February 2016

positive mode, occurring at m/z +206, +207 and +208. Other peaks in the positive ion spectrum include m/z 23 $[Na]^+$, m/z 56 $[Fe]^+$, m/z 39 and 113 ($[K]^+$and $[K_2Cl]^+$). In addition to nitrate (m/z -46 $[NO_2]^-$ and m/z -62 $[NO_3]^-$), chloride (m/ -35 ($[Cl]^-$) was one of the most abundant species in the negative ion mode. A similar particle type containing lead and chloride (Pb-Cl) was detected by ATOFMS in Mexico City and attributed to a waste incinerator source (Moffet et al., 2008), although other studies in the same area attributed lead-containing particles to multiple sources, including trash burning (Salcedo et al., 2010; Hodzic et al., 2012). This ATOFMS particle type was found highly correlated with hourly elemental concentrations determined by PIXE analysis (Dall´Osto et al., 2013), showing that this source of Pb-Cl is a major (82%) source of fine Cl in the urban agglomerate of Barcelona. It is worth noting that whilst the regional particle type Fe was mainly distributed in the fine mode (about 300-500 nm), a much larger mode (about 700-900 nm) was observed for this local ATOFMS Pb particle type (see Fig. SI 2 d). Finally, the temporal trend (Fig. S1d) and the diurnal profile (Fig. 3) of the Pb particle type also suggests a local origin, likely related to emissions from urban combustion.

3.3 particle types observed at UB

The ATOFMS fitted with converging nozzle inlet located at the UB site detected four particle types that were not observed at the RS site. Each of the particle types make a minor contribution (0.9-1.7%) and overall they represented less than 5% of the total particles sampled at the UB site.

Atmos. Chem. Phys. Discuss., doi:10.5194/acp-2015-986, 2016
Manuscript under review for journal Atmos. Chem. Phys.
Published: 5 February 2016

Atmospheric Chemistry and Physics Discussions

3.3.1 Vanadium-containing particles (V)

A particle type containing vanadium (m/z 51 $[V]^+$ and m/z 67 $[VO]^+$) Na (m/z 23) and Fe (m/z 56), along with minor peaks due to EC at m/z 36, 48 and 60 was observed at the UB site. A negative ion mass spectrum was not acquired for this particle type, Figure 4a. It has been shown that the condensation of secondary material on soot particles (Moffet and Prather, 2009) and the consequent change in aerosol hygroscopicity (Spencer et al., 2007) can suppress the formation of negative ions in real-time laser desorption/ionisation mass spectrometry, causing many aged EC-containing particles to lack negative mass spectra (Neubauer et al., 1998). The V particle type accounted for only 1% of the particles characterised at the UB, with a unimodal distribution peaking at about 350 nm pointing to a fresh combustion emission source. Field observations have confirmed that ships produce significant amounts of soot, vanadium, nickel, and sulfate (Pattanaik et al., 2007). Previous ATOFMS field measurements also reported that single particles containing organic carbon, vanadium, and sulfate (OC-V-sulfate) resulted from residual fuel combustion (i.e. bunker fuel), whereas high quantities of fresh soot particles represented distinct markers for plumes from distillate fuel combustion (i.e. diesel fuel) from ships as well as trucks in the port area (Healy et al., 2009; Ault et al., 2010). Indeed, the V particle type presented a temporal variation showing a maximum on 3 October 2010, when strong wind was blowing from the port of Barcelona (North African tropical air masses from West, NAF_W, Fig. SI 1 e). This Vanadium particle type is therefore most likely associated with fuel oil and ship emissions from the port. However, it was not detected at the RS site, possibly due to local street canyon effects which restrict transport and mixing in the area (Solazzo et al., 2008).

Atmos. Chem. Phys. Discuss., doi:10.5194/acp-2015-986, 2016
Manuscript under review for journal Atmos. Chem. Phys.
Published: 5 February 2016

3.3.2 Soil rich in Ca (Soil-Ca)

The average ATOFMS mass spectrum of a dust particle type rich in calcium is shown in Fig. 4b, where peaks for calcium (m/z 40 $[Ca]^+$, 56 $[CaO]^+$, 57 $[CaOH]^+$ and 96 $[Ca_2O]^+$) are present. Peaks associated with sodium (m/z 23), magnesium (m/z 24, 25) and potassium (m/z 39) can also be seen. The Soil-Ca particle class represented 0.9% of the particles sampled at the UB site and was found to moderately correlate (R^2=0.6) with the urban Dust (Ca) factor obtained by PIXE-PMF analysis (Dall´Osto et al., 2013). The large aerosol size mode above 1 µm (Fig. SI 1e) also points a dust origin. Enhanced levels of the Ca ATOFMS particle type were observed during Atlantic (ATL) air masses (Dall´Osto et al., 2012), likely due to extra resuspension of dust caused by the high wind speeds during these periods. Urban areas in the South of Europe are known to have high dust loadings and three different types of dust were previously reported in the SAPUSS PIXE study (Dall´Osto et al., 2013), representing ca. 25% of the $PM_{2.5}$ mass concentrations measured. It should be noted that this particle type did not possess a negative ion mass spectrum and was also not detected at the RS site, likely for the same reasons explained above (section 3.3.1).

3.3.3 Saharan dust particles (Saharan-dust)

A rarely observed particle type with peaks due to titanium at m/z 48 and m/z 64 ($[Ti]^+$ and $[TiO]^+$, respectively) was found to represent 0.9% of the particles sampled at the UB site (Fig. 4c). Additional peaks are associated with other metals including Na (m/z

Atmos. Chem. Phys. Discuss., doi:10.5194/acp-2015-986, 2016
Manuscript under review for journal Atmos. Chem. Phys.
Published: 5 February 2016

23), Al (m/z 27), Ca (m/z 40, 56, 96) and Fe (m/z 56), as well as minor peaks of silicate at m/z - 60 $[SiO_2]^-$ and - 76 $[SiO_3]^-$. These particles presented an aerosol size coarse mode (1-3µm; Fig. SI2) and were detected mainly during the period 8-10 October, when Barcelona experienced air masses originating in the North African Saharan region (Dall´Osto et al., 2012). This particle type was likely not detected at the RS site because the ATOFMS fitted with the aerodynamic focussing lens is not efficient at detecting such coarse particles. With regard to secondary species, it is interesting to note that the dust was internally mixed only with nitrate and not with sulfate (Fig. 4c). Previous studies (Dall´Osto et al., 2010) showed that Saharan dust particles collected near the Cape Verde Islands contained internally mixed nitrate but no sulfate, whilst Saharan dust particles collected on the coast of Ireland showed a very high degree of internally mixed secondary species including nitrate, sulfate and methanesulfonate (Dall´Osto et al., 2004).

3.3.4 Vegetative debris (Veg-KP)

The ATOFMS has already proven to be a good tool for identifying and separating dust (mainly Ca-rich or Al-Si rich) and biological particles (Fergenson et al. 2004). A particle type dominated by K (m/z 39) and phosphate (m/z -63 and m/z - 79) in the average mass spectrum (Fig. 4d) accounted for 1.7% of the total particles sampled at the UB site. Strong signals at m/z 26 and m/z 42, due to $[CN]^-$ and $[CNO]^-$ are also present, as well as peaks due to Na (m/z 23) and Fe (m/z 56) . A coarse aerosol size mode of about 3 µm (Fig. SI2) is likely again the reason why this particle type was not detected by the ATOFMS at the RS site. The size and chemical composition

Atmos. Chem. Phys. Discuss., doi:10.5194/acp-2015-986, 2016
Manuscript under review for journal Atmos. Chem. Phys.
Published: 5 February 2016

suggest a source such as vegetative debris and the particle type is thus labelled Veg K-P. A previous ATOFMS study reported a very similar particle type from samples of leaves collected from a roadside (Schofield, 2004). It is interesting to note that an increase of this vegetative debris particle type was detected under NAF_W air masses in concomitance with Saharan dust particles. Previous atmospheric measurements have shown that the concentration of bacteria over the sea may be much lower than over land, but that higher concentrations of aerosolized microorganisms are generated during dust events compared to clean background marine conditions (Kellog and Griffin 2006, Prospero et al., 2006).

3.4 particle types observed at RS

The ATOFMS fitted with an aerodynamic focussing lens located at the RS site detected 8 particle types that were not observed at the UB site.

3.4.1 Amines

Amines are ubiquitous in the atmospheric environment, and have been detected in marine, urban and rural atmosphere in the gas and particle phases as well as aqueous fog and rain water (Ge et al., 2011). The ATOFMS is a particularly good aerosol instrument for studying amines because the LDI laser wavelength (266 nm) ionizes them very efficiently (Angelino et al., 2001; Healy et al., 2015). During the SAPUSS measurement campaign, four amine particle types were detected at the RS. To the best of our knowledge, this is the first time such a variety of organo-

Atmos. Chem. Phys. Discuss., doi:10.5194/acp-2015-986, 2016
Manuscript under review for journal Atmos. Chem. Phys.
Published: 5 February 2016

nitrogen particle types has been detected at the single particle level in real time in urban air.

(a) *Amine (Traf. 58):* Fig. 5a shows the ATOFMS mass spectra of a particle type called Amine-58; which accounted for 0.8% of the total particles classified at RS. The strongest peak in the positive mass spectra at m/z 58 is likely due to $[C_2H_5NH{=}CH_2]^+$. In general, the most important primary fragmentation process occurring for aliphatic amines involves the removal of one of the electrons from the lone pair on N and cleavage of the C-C bond to the nitrogen, with loss of the heavier alkyl group favoured. This cleavage explains the presence of the fragments at m/z 58 $[C_2H_5NH{=}CH_2]^+$, 72 $[C_3H_7NH{=}CH_2]^+$, 86 $[(C_2H_5)_2N{=}CH_2]^+$, and 114 $[(C_3H_7)_2N{=}CH_2]^+$. The minor peak at m/z 86 was found to correlate (R^2 = 0.8) with m/z 58. M/z 86 was suggested as amine species associated with fresh mobile emissions (Angelino et al., 2001). The negative mass spectrum shows nitrate and sulfate internally mixed with this particle type, although the former has a stronger signal than the latter. A size distribution peaking at about 300-400 nm was associated with this particle type. The diurnal variation of Amine (Traf. 58) (Fig. 6a) shows a peak about one hour later than morning and evening rush hour trafficand thus points to relatively fresh vehicular source. In conclusion, both the mass spectra (similar to previous traffic emissions, Angelino et al., 2001) and the temporal trend of this particle type point to traffic emission as a main source.

(b) *Amine (ETS. 84)* Fig. 5b shows the average mass spectrum of a particle type associated with Environment Tobacco Smoke (ETS) called Amine-84, which

Atmos. Chem. Phys. Discuss., doi:10.5194/acp-2015-986, 2016
Manuscript under review for journal Atmos. Chem. Phys.
Published: 5 February 2016

represented 0.5% of the total particles classified at RS. In the positive mass spectrum, the peak at m/z 161 is assigned to nicotine, with the main fragment being at m/z 84 (methyl-pyrrole fragment). The negative mass spectrum shows nitrate and sulfate internally mixed with this particle type. The Amine-84 mass spectrum is very similar to that previously reported in Athens (R^2 = 0.9; Dall´Osto et al., 2007) and also attributed to tobacco smoke. This particle type generally followed human activity within the city (Fig. 6a), with a main peak in the morning (10 am) and a broader one during the evening (6pm -10 pm). It should be noted that an afternoon peak - potentially related to lunch activites - was not noticed. Spain ranks among the countries with the highest levels of cigarette consumption in the European Union and in the World (WHO, 2010; Ailer et al.; 2013). High outdoor gas-phase nicotine concentrations (0.5 and 1.5 µg m^{-3}) have been previously measured in Barcelona in summer 2010 (Sureda et al., 2012).

(c) *Amine (SOA 59):* Figure 5c shows the average mass spectrum of a particle type called amine-59, which accounted for 0.2% of the total particles classified at RS. Based on previous studies, the strong peak at m/z 59 ($[N(CH_3)_3]^+$) is attributed to Trimethylamine (TMA) (Angelino et al., 2001; Zhuang et al., 2012; Healy et al., 2015). Amine (SOA 59) concentration was found particularly enhanced under regional air masses (13-17 October 2010, Fig. SI 1 h) and exhibited a diurnal trend (Fig. 6a) showing maximum concentrations at 3 pm and 10 pm. TMA plays an important role in atmospheric chemistry, yet its pathway towards aerosol is not clear. Rehbein et al. (2011) demonstrated that cloud/fog processing could enhance gas-to-particle partitioning of TMA. TMA can also participate in the formation of secondary organic

Atmos. Chem. Phys. Discuss., doi:10.5194/acp-2015-986, 2016
Manuscript under review for journal Atmos. Chem. Phys.
Published: 5 February 2016

aerosol. Several studies have shown that gas-phase TMA could form non-salt organic aerosol products through reaction with oxidizing agents (Murphy et al., 2007).

(d) *Amine (SOA 114)*: Fig. 5d shows the average mass spectrum for a particle type called amine (SOA 114). The main peak is at m/z 114, which may be assigned to dipropylamine or tripropylamine (Angelino et al., 2001; Healy et al., 2015). Minor peaks can also be seen at m/z 58, 74 and 128, which were previously attributed to alkyl ammonium nitrate salt particles formed by reaction of nitic acid and amines (Angelino et al., 2001). The negative ion mass spectrum for Amine (SOA 114) shows a strong peak at m/z -62, confirming the presence of nitrate. Fig. 6a shows that the diurnal profile is similar to that reported for Amine (SOA 59), although with a much stronger peak at 3 pm, during the warmest part of the day for the measurment period (Dall´Osto et al., 2013). This is in line with recent measurements of gaseous amines by ambient pressure proton transfer mass spectrometry (Hanson et al., 2011) which also showed anenhancement of TEA (triethylamine) during the afternoon. Amine (SOA 59) and Amine (SOA 114) presented similar diurnal profiles but their temporal occurence was not similar. Whilst Amine (SOA 59) was detected mainly during the period of nitrate-rich regional air masses (13-17 October), Amine (SOA 114) was detected mainly under NAF_E air masses rich in sulphate (7-10 October 2010). This observation is discussed further in section 4.

Overall, the four amine containing particle types were found distributed mainly in the sub micron mode. Amine (Traf. 58) and Amine (ETS 84), which are attributed to primary emissions from traffic and ETS respectively, have similar size distributions

Atmos. Chem. Phys. Discuss., doi:10.5194/acp-2015-986, 2016
Manuscript under review for journal Atmos. Chem. Phys.
Published: 5 February 2016

which peak around 400-500 nm (Fig. SI 2). Amines (SOA 59) and Amine (SOA 114) were also found in the same size range, but presented a broader shape, suggesting partial condensation of SOA material on existing particles. Previous work of Angelino et al. (2001) used the peak at m/z 118 to track a marker for the oxidation products of alkylamines observed in the condensed phase of aerosol particles, specifically attributed to the oxidation of triethylamine (m/z 118; $[(C_2H_5)_2NCH_2]^+$). The analysis of the ATOFMS dataset for the RS site shows that the majority (about 80%) of amine particle types containing a peak at m/z 118 was found in the tobacco related ATOFMS Amine (ETS 84) class, whereas the remaining 20% was associated with Amine (Traf. 58). This suggests - at least in our study - that m/z 118 cannot be used ly as marker amines produced by secondary processes. Other possible identification of higher mass ions detected and associated with organic nitrate include m/z 74 ($[C_2H_4NO_2]^+$), 88 ($[C_3H_6NO_2]^+$ or $(([C_2H_5)_2NO]^+$), 104 ($[C_3H_6NO_3]^+$), and 191($[C_6H_{11}N_2O_5]^+$). Overall, m/z 104 was found to be to Amine (Traf. 58), whereas m/z 74 and m/z 191 to Amine (SOA 114). Finally, m/z 88 was found associated with both Amine (Traf. 58) and Amine (SOA 114). In summary, organic nitrate peaks were associated with both primary and secondary amine particle types.

3.4.1 Organic Carbon (OC) particle types

The high efficiency of the ATOFMS equipped with the aerodynamic lens and deployed at the RS allowed us to characterise four particle types rich in organic compounds.

Atmos. Chem. Phys. Discuss., doi:10.5194/acp-2015-986, 2016
Manuscript under review for journal Atmos. Chem. Phys.
Published: 5 February 2016

(a) *Org (Lub. Oil)*: Fig. 7a shows the average mass spectrum of a particle type named "Lub. Oil" (1.8%). The positive ion mass spectrum shows strong peaks for $[Ca]^+$ (m/z 40), and minor ones for OC (m/z 27, 43, 57) and EC (m/z 12, 24, 36, 48, 60). The negative mass spectra shows presence of nitrate (m/z -46, -62) and EC (-36, -48, -60). This particle type was only detected in the lower size range of the ATOFMS (ca. 150-400 nm), was found to spike during traffic rush hour times (Fig. 6b) and is attributed to lubricating oil from traffic emissions (Spencer et al., 2006; Drewnick et al., 2008).

(b) Org. (*Aro-NIT)*: A particle type rich in aromatic compounds and internally mixed with nitrate (Org. (Aro-NIT)) was found to account for 1.7% of the particles classified at the RS. The average mass spectrum shown in Fig. 7b features strong signals due to organic fragments at m/z 27, 29, 39, 43, 51, 57 and 63. M/z 51 $[C_4H_3]^+$, 63 $[C_5H_3]^+$, 77 $[C_6H_5]^+$ and 91 $[C_7H_7]^+$ are indicative of a strong aromatic signature (McLafferty, 1993). Common peaks due to nitrate (i.e. m/z -46 $[NO_2]^-$, m/z -62 $[NO_3]^-$) are found in the negative mass spectrum. Fig. 6b shows a daily maximum of this particle type at about 7-8 pm. Two previous ATOFMS studies in Athens (Dall´Osto and Harrison, 2006) and London (Dall´Osto and Harrison, 2012) reported very similar particle types (called C-SEC_2 and Na-EC-OC, respecively) which were attributed to condensation of organic compounds onto the particle phase as air temperatures dropped. The secondary particles showed clear internal mixing of organic and inorganic constituents. The size distribution of the Aro-NIT particle type shows a broad mode at about 500-700 nm (Fig. SI 2), also suggesting condensation of species on existing aerosols.

Atmos. Chem. Phys. Discuss., doi:10.5194/acp-2015-986, 2016
Manuscript under review for journal Atmos. Chem. Phys.
Published: 5 February 2016

Atmospheric Chemistry and Physics Discussions

(c) Org. (*OC-NIT)*: A third organic-rich particle type, called OC-NIT (1.5% of the particles classified), was also detected at the RS site. Fig. 7c shows the average positive ion mass spectrum, which contains a strong peak at m/z 39 (K and/or C_3H_3) and minor peaks due to OC and EC, as well as Na (m/z 23). Perhaps the most intersting part of the negative spectrum for this particle type is the presence of signals due to organic nitrogen species (m/z -26 $[CN]^-$ and m/z -42 $[CNO]^-$), not seen in other organic rich particle types shown in Fig. 7. Finally, strong peaks for nitrate (m/z -46, -62) dominate the negative mass spectra. Fig. 6b shows a daily maximum concentration of OC-NIT at 3 pm. The presence of an organo nitrogen component in this particle type, as well as its maximum at 3 pm, is similar to that for the Amine (SOA 59) particle type described in the previous section.

(d) Org. (*OC-CHO)*: This particle type presents a positive mass spectrum (Figure 7d), with strong peaks at m/z 27 $[C_2H_3]^+$ and m/z 43 $[(CH_3)CO]^+$ usually associated with oxidized secondary organic aerosol (Sullivan and Prather, 2005). Peaks at m/z 29 $[C_2H_5]^+$ and m/z 41 $[C_3H_5]^+$ confirm the strong hydrocarbon-like nature of the particles (Spencer et al., 2006), while weak peaks at m/z 51 $[C_4H_3]^+$, 63 $[C_5H_3]^+$, 77 $[C_6H_5]^+$ and 91 $[C_7H_7]^+$ also indicate an aromatic contribution (McLafferty, 1993). A negative ion mass spectrum was often not recorded for this particle type. However, some of the particles did generate one and an example is shown in Fig. SI 3 d. The presence of peaks at m/z –45, –59 and –71 are likely to be due to the formate $[CHO_2]^-$, acetate $[C_2H_3O_2]^-$ and propionate $[C_3H_5O_2]^-$ ions, respectively. Figure 6b shows that in contrast to the other three OC-rich particle types, OC-CHO shows a

Atmos. Chem. Phys. Discuss., doi:10.5194/acp-2015-986, 2016
Manuscript under review for journal Atmos. Chem. Phys.
Published: 5 February 2016

complex diurnal profile. The number of counts per hour increases from 6-8 am and then remains stable for about 5 hours. A peak is observed around 3 pm, the hottest part of the day, followed by a second peak at about 10-11pm. This diurnal profile is similar to that of Amine (SOA 114) , which is also of secondary origin.

Overall these four OC-rich particle types indicate that a number of processes and sources are likely producing oxidised organic aerosols. There are at least four main peaks during the day: a morning traffic rush hour (9-10 am), an afternoon one during the hottest part of the day (3 pm), and two evening ones at 8 pm (sun set) and at about 10-11pm.

4. Discussion and conclusions

During the SAPUSS intensive field study two ATOFMS instruments were deployed simultaneously. The ATOFMS deployed at the RS site was equipped with an aerodynamic lens inlet system, allowing characterisation of primary traffic aerosols as well as other primary and secondary aerosols affecting this heavily urbanised area of Barcelona. This type of ATOFMS (Su et al., 2004) has a very high efficiency in sampling aerosols (more than 1,000,000 single particle mass spectra were collected at the RS), particularly for sub micron particles in the size range 300-700 nm. The ATOFMS deployed at the UB site was equipped with a converging nozzle inlet system (Gard et al., 1997), which has a low aerosol collection efficiency (Dall´Osto et al., 2006) but it is particularly well suited for sampling coarser aerosols in the size range 800-2000 nm.

Atmos. Chem. Phys. Discuss., doi:10.5194/acp-2015-986, 2016
Manuscript under review for journal Atmos. Chem. Phys.
Published: 5 February 2016

Atmospheric Chemistry and Physics Discussions

Overall, ten particles types were detected at both sites (Table 1). Two of these particle types, composed of EC internally mixed with secondary inorganic species, described more than half of the classified single particle mass spectra. EC_aged_R. was found accumulating within stagnant air masses, with a flat diurnal profile and suggesting a certain physico-chemical stability. In contrast, a more local but processed form of EC (EC_aged_L.) was found to possess a finer submicron mode, and enhanced concentrations during afternoon periods.

Two different types of nitrate-dominated aerosols were observed, in line with a previous ATOFMS study in London (Dall´Osto et al., 2009). The first (LRT_NIT) was attributed to regional nitrate (accumulation mode, volatile, more NH_4NO_3/ $(NH_4)_2SO_4$ type) and the second (Loc_NIT) was assigned to local nitrate (ultrafine mode, less volatile, more OC-NO_3 type). An enhancement of local nitrate was found under warm and humid NAF_E air masses, indicating that meteorological conditions (i.e. high RH) or aerosol composition (i.e. sea salt, Saharan dust) could affect local urban nitrate aerosol production.

Two types of sea salt particles were also identified at both sites. Fresh sea salt particles (NaCl) showed a peak in the diurnal profile at 3 pm, related to the sea breeze and enhanced under NAF_E air masses. Aged sea salt particles (NaCl-NIT) were mainly observed during more anthropogenically influenced air masses.

Two types of particles rich in metallic elements were found at both monitoring sites. One, rich in iron and internally mixed with nitrate, was found to be distributed in the fine accumulation mode at about 400 nm and related to regional air masses. This observation supports previous findings (Dall´Osto et al., 2010, Harrison et al., 2012) that showed fine iron-containing aerosols are able to travel long distances and are

Atmos. Chem. Phys. Discuss., doi:10.5194/acp-2015-986, 2016
Manuscript under review for journal Atmos. Chem. Phys.
Published: 5 February 2016

thus related to aged air masses. Other studies have reported anthropogenic Fe-containing particles internally mixed with secondary species such as sulfate (Furutani et al., 2011; Moffet et al., 2012) originating from coal combustion in Asian continental outflows. This study shows that - within the European continental outflow - Fe-containing particles are instead internally mixed with nitrate. This observed difference is likely due to emissions from coal combustion in Asia which are rich in SO_2, as opposed to European air masses which are relatively higher in NO_2 and lower in SO_2. Bio-available iron from atmospheric aerosol is an essential nutrient that can control ocean productivity (Baker and Croot, 2010). Hence, it can impact the global carbon budget and climate. There are also large uncertainties in the origin of the aerosol nitrogen matter which may be enhancing ocean productivity (Duce et al. 2008). The fact iron is internally mixed with nitrate points to an urban source (i.e. more traffic than industrial activities), suggesting transported submicron urban particles can be a source of both iron and nitrogen nutrients for the oceans. However, it is worth noting that Cu-rich traffic related aerosols can also have a negative effect on marine phytoplankton over a vast region of the western Mediterranean Sea (Jordi et al., 2012).

A second metallic particle type rich in lead and chloride was identified. This particle type was related to more local sources, presenting sharp spikes in concentration. It is interesting to note this particle type was found correlated with hourly elemental mass concentrations determined by PIXE analysis (Dall´Osto et al., 2013) showing this particle type can be a major source of submicron chloride in the urban area of Barcelona.

Atmos. Chem. Phys. Discuss., doi:10.5194/acp-2015-986, 2016
Manuscript under review for journal Atmos. Chem. Phys.
Published: 5 February 2016

Atmospheric Chemistry and Physics Discussions

The ATOFMS equipped with the converging nozzle inlet at the UB site detected four further different particle types. Two types of dust particles were found, both occurring mainly in the coarse mode (>1 μm): one type, as attributed to Saharan Dust, was characterized by an aluminium/silicon signature, while the other type, with a more local origin (Ca dust), was characterized by a Ca-rich composition. Two other minor coarse particle types were characterised: vegetative debris (Veg-KP, rich in potassium and phosphate), found enhanced during tropical NAF_E air masses; and vanadium-containing particles (Oil-V), and related to shipping/oil combustion activities in the port of Barcelona. Overall, high concentrations of vanadium were only observed on one day (3 October), indicating that shipping emissions was a minor source of aerosol at the UB site.

Eight particle types were detected by the ATOFMS with aerodynamic focussing lens at the RS site. Overall, these particle types described less than 10% of the aerosol population, but their mass spectra, as well as their peculiar diurnal profiles, allow us to advance our understanding of the OC-ON-Nitrate mixing state of urban aerosols.

Four particle types contain amines, which, in addition to ammonia, are important atmospheric bases (Ge et al., 2011). Urban concentrations of ammonia in Barcelona are higher than those reported in similar urban background sites in Europe, especially in summer (Reche et al., 2012). Conversely, in winter, levels of ammonia were higher at traffic-affected sites, suggesting a contribution from vehicle emissions (Reche et al., 2012). In comparison, the sources, atmospheric transformation and sinks of amines are more poorly characterised. Overall, both primary (Amine Traf. 58 and Amine ETS 84) and secondary (Amine SOA 59 and Amine SOA 114) sources of amine-containing particles were identified during SAPUSS. The most abundant

Atmos. Chem. Phys. Discuss., doi:10.5194/acp-2015-986, 2016
Manuscript under review for journal Atmos. Chem. Phys.
Published: 5 February 2016

amine particle type (Amine Traf. 58, 0.8% of total particles at RS) was attributed to traffic activities and the second most abundant (Amine ETS 84, 0.5% of the total particles at RS) was also associated with environmental tobacco smoke. Concurrent SAPUSS measurements (Alier et al., 2013) of nicotine concentrations were much higher at the RS site (58 ng m^{-3}) than at UB (7 ng m^{-3}), pointing to a significant outdoor cigarette consumption in the city centre. A recent study (Sleiman et al., 2010) found that nicotine can contribute significantly to the formation of urban SOA though reaction with ozone. The results of this study therefore suggest that third-hand cigarette smoke may be a source of nitrogen-containing particles in Barcelona and similar cities in Southern Europe where smoking is prominent.

Amines were also related to secondary aerosol production, although a very complex dynamic was found associated with their occurrences. They were found to peak during the warmest part of the day (3 pm) and during evening times (10-11 pm). Amine (SOA 59), was found particularly enhanced in regional air masses (13-17 October 2010) when nitrate concentrations were also high (Dall´Osto et al., 2013). By contrast, Amine (SOA114) was more abundant in NAF_E humid air masses (7-11 October 2010). This latter type of SOA had was internally mixed with nitrate, suggesting aminium salt formation under such specific conditions. Previous ATOFMS studies reported that most of the amines volatilised during cold seasons, whereas during summer most were in the form of low-volatility aminium nitrate and sulphate salts when particle acidity was higher (Pratt et al., 2009); supporting laboratory studies reporting that aerosol containing non-salt organic amines are more stable than nitrate salts (Murphy et al., 2007). Overall, amines can undergo oxidation by OH, O_3, and/or NO_3 to form amides, nitramines, and imines, which can also partition to the particle phase (Murphy et al., 2007; Silva et al., 2008, Healy et al., 2015).

Atmos. Chem. Phys. Discuss., doi:10.5194/acp-2015-986, 2016
Manuscript under review for journal Atmos. Chem. Phys.
Published: 5 February 2016

Rehbein et al. (2011) combined field and laboratory work to demonstrate that high relative humidity greatly enhances the gas-to-particle partitioning and subsequent aqueous acid–base reaction of amines. During the SAPUSS study, we find aminium nitrate salts on coarse particles containing sulfate, suggesting that heterogeneous reactions occur during the warmest part of the day. This observation is in contrast to the study of Day et al. (2010), who reported organo-nitrates when sulfate aerosols and humidity were low, although the study site was less urbanised than the one used in this study.

Finally, some consideration should be given to the four specific organic particle types detected at the RS. One (Org. (Lub. Oil)) was found to be related to primary lubricating oil traffic emissions. More difficult is the attribution of the remaining three, which each contain an internal mixture of OC and nitrate. This is not surprising, given the fact the urban atmosphere is heavily contaminated by traffic emissions, the main producers of the two chemical species (Dall´Osto et al., 2012a).

Two different types of organic carbon / nitrate particle types were found. One (OC-NIT) was found spiking in the afternoon. By contrast, a nitrate with a strong aromatic signature (OC-Aro-NIT) was found mainly during night time (80% of the time), and showing a sharp concentration peak at 7-8 pm. These two ATOFMS particle types add complexity to the local-regional inorganic nitrate containing particle types, and further studies are needed to correctly apportion the local urban nitrate component.

The fourth organic particle type (OC-CHO) was found rich in oxidised organic carbon and associated with nitrate from a traffic source. In a previous ATOFMS study, considerable effort was made to apportion cooking-related particle types (Dall´Osto and Harrison, 2012). However, only a particle type exhibiting maximum frequency

Atmos. Chem. Phys. Discuss., doi:10.5194/acp-2015-986, 2016
Manuscript under review for journal Atmos. Chem. Phys.
Published: 5 February 2016

Atmospheric Chemistry and Physics Discussions

during the warmest part of the day and associated with secondary aerosol production from traffic-related semi-volatile aromatic compounds was found. During this study, we were again not able to associate a specific particle type with cooking activities. In a companion SAPUSS study, Alier et al. (2013) reported an aerosol source formed mainly by C_7-C_9 dicarboxylic acids and detected especially during daytime, highly dynamic, dependent on air masses and pointing to a secondary organic component driven by primary urban sources including cooking and traffic (mainly gasoline) activities. O`Brien et al. (2013) reported a detailed mass spectrometry characterisation of the urban aerosol in an urban background environment. Compounds containing only carbon, hydrogen, and oxygen (CHO), and nitrogen-containing organic compounds (NOC) were found, showing that both photo-oxidation and ammonia chemistry may play a role in forming the compounds observed in the mixed urban-rural environment. NOC had precursor product pairs consistent with imidization and cyclization reactions, suggesting that part of the aromatic compounds detected during SAPUSS may also be formed by cyclization and not only by condensation of aromatic VOC.

In summary, the two ATOFMS instruments deployed during the SAPUSS field measurement study showed that the urban atmosphere contains a complex mixture of aerosol particles emitted from a variety of sources and formed via numerous atmospheric processes. We have identified 22 different particle types, characterised by specific single particle mass spectra and temporal trends. Particle composition is strongly affected by the prevailing air masses. The ATOFMS measurements also provided some novel information on the mixing state of organic carbon and nitrate in

urban aerosols, again highlighting the complex nature of the roles played by both primary sources and in situ chemical processing in affecting aerosol composition.

Acknowledgements

Financial support for this study was provided by the Marie Curie FP7 SAPUSS (FP7-PEOPLE-2009-IEF, Project number 254773), and previously supported by research projects from the D.G. de Calidad y Evaluacion Ambiental (Spanish Ministry of the Environment) and the Plan Nacional de IyD (Spanish Ministry of Science and Innovation) CGL2010-19464- VAMOS, CTQ2009-11572 and CTQ2009-377-14777-C02-01-AERTRANS). The SAPUSS team is also acknowledged.

References

Abbatt J. P. D., Leea, A. K. Y. and Thornton J.A. Quantifying trace gas uptake to tropospheric aerosol: recent advances and remaining challenges. Chem. Soc. Rev., 2012, 41, 6555–6581, 2012

Alier, M., van Drooge, B. L., Dall'Osto, M., Querol, X., Grimalt, J. O., and Tauler, R.: Source apportionment of submicron organic aerosol at an urban background and a road site in Barcelona (Spain) during SAPUSS, Atmos. Chem. Phys., 13, 10353-10371, doi:10.5194/acp-13-10353-2013, 2013.

Allan, D., Williams, P.I., Morgan, W.T., Martin, C.L., Flynn, M.J., Lee, J., Nemitz, E., Phillips, G.J., Gallagher, M.W., Coe, H.: Contributions from transport, solid fuel

burning and cooking to primary organic aerosols in two UK cities, Atmos. Chem. Phys. 10, 2, 647-668, 2010.

Angelino, S.; Suess, D. T.; Prather, K. A. Formation of aerosol particles from reactions of secondary and tertiary alkylamines: Characterization by aerosol time-of-flight mass spectrometry. Environ. Sci. Technol, 35 (15), 3130–3138, 2001.

AQEG (2005). "Particulate matter in the UK." Defra, London.

Ault, A. P., Gaston, C. J., Wang, Y., Dominguez, G., Thiemens, M. H., and Prather, K. A.: Characterization of the Single Particle Mixing State of Individual Ship Plume Events Measured at the Port of Los Angeles, Environ. Sci. Technol., 44, 1954–1961, doi:10.1021/es902985h, 2010.

Baker, A. Croot. P. L. Atmospheric and marine controls on aerosol iron solubility in seawater, Marine Chemistry, 120, 4-13, 2010.

Benton, A. K., Langridge, J. M., Ball, S. M., Bloss, W. J., Dall'Osto, M., Nemitz, E., Harrison, R. M., and Jones, R. L.: Night-time chemistry above London: measurements of NO3 and N2O5 from the BT Tower, Atmos. Chem. Phys., 10, 9781-9795, doi:10.5194/acp-10-9781-2010, 2010

Brown, S. S., deGouw, J. A.,Warneke, C., Ryerson, T. B., Dube,W. P., Atlas, E., Weber, R. J., Peltier, R. E., Neuman, J. A., Roberts, J. M., Swanson, A., Flocke, F., McKeen, S. A., Brioude, J., Sommariva, R., Trainer, M., Fehsenfeld, F. C., and Ravishankara,A. R.: Nocturnal isoprene oxidation over the Northeast United States in summer and its impact on reactive nitrogen partitioning and secondary organic aerosol, Atmos. Chem. Phys., 9, 3027–3042, doi:10.5194/acp-9-3027-2009, 2009.

Canagaratna, M. R., Jayne, J. T., Jimenez, J. L., Allan, J. D., Alfarra, M. R., Zhang, Q., Onasc, T. B., Drewnick, F., Coe, H., Middlebrook, A., Delia, A., Williams, L. R., Trimborn, A. M., Northway, M. J., DeCarlo, P. F., Kolb, C. E., Davidovits, P. and Worsnop D. R.: Chemical and microphysical characterization of ambient aerosols with the aerodyne aerosol mass spectrometer, Mass Spectrom. Rev., 26, 185–222, 2007.

Dall'Osto, M., Beddows, D.C.S., Kinnersley, R.P., Harrison, R.M., Donovan, R.J. and Heal M.R. Characterization of individual airborne particles by using Aerosol Time-of-Flight Mass Spectrometry (ATOFMS) at Mace Head, Ireland. Journal of Geophysical Research 109, D21302, doi: 10.1029/2004/JD004747, 2004.

Dall'Osto, M., Harrison, R. M., Beddows, D. C. S., Freney, E. J., Heal, M. R. and Donovan R. J.: Single-particle detection efficiencies of aerosol time-of-flight mass spectrometry during the North Atlantic marine boundary layer experiment, Environ. Sci. Technol., 40, 5029-5035, 2006.

Dall'Osto, M. and Harrison R. M.: Chemical Characterisation of single airborne particles in Athens (Greece) by ATOFMS, Atmos. Environ., 40, 7614-7631, 2006.

Dall'Osto, M., R. M. Harrison, E. Charpantidou, G. Loupa and S. Rapsomanikis. "Characterisation of indoor airborne particles by using real-time aerosol mass spectrometry." Science Of The Total Environment 384(1-3): 120-133, 2007.

Dall'Osto,M.; R. M. Harrison, E. J. Highwood, C. O'Dowd, D. Ceburnis, X. Querol, E. P. Achterberg, Variation of the mixing state of Saharan dust particles with atmospheric transport, Atmospheric Environment, Volume 44, Issue 26, 3135-3146, ISSN 1352-2310, DOI: 10.1016/j.atmosenv.2010.05.030, 2010.

Dall'Osto, M., Harrison, R. M., Coe, H., Williams, P. I., and Allan, J. D.: Real time chemical characterization of local and regional nitrate aerosols, Atmos. Chem. Phys., 9, 3709-3720, 2009.

Dall'Osto, M., Querol, X., Alastuey, A., Minguillon, M. C., Alier, M., Amato, F., Brines, M., Cusak, M., Grimalt, J. O., Karanasiou, A., Moreno, T., Pandolfi, M., Pey, J., Reche, C., Ripoll, A., Tauler, R., Van Drooge, B. L., Viana, M., Harrison, R.M.,Gietl, J., Beddows, D., Bloss, W., O'Dowd, C., Ceburnis, D., Martucci, G., Ng, S., Worsnop, D., Wenger, J., Mc Gillcuddy, E., Sudou, J., Healy, R., Lucarelli, F., Nava, S., Jimenez, J.L., Gomez Moreno, F., Artinano, B., Prevot, A.S., Pfaffenberger, L., Frey, S., Wilsenack, F., Casabona, D., Jimenez-Guerrero, P., Gross, D., Cotz, N.: Presenting SAPUSS: Solving Aerosol Problem by using synergistic strategies at Barcelona, Spain, Atmos. Chem. Phys. Discuss., 12, 18741-18815, 2012a.

Dall'Osto, M. and Harrison, R. M.: Urban organic aerosols measured by single particle mass spectrometry in the megacity of London, Atmos. Chem. Phys., 12, 4127-4142, doi:10.5194/acp-12-4127-2012, 2012b.

Dall'Osto, M., Querol, X., Amato, F., Karanasiou, A., Lucarelli, F., Nava, S., Calzolai, G., and Chiari, M.: Hourly elemental concentrations in PM2.5 aerosols sampled simultaneously at urban background and road site during SAPUSS – diurnal variations and PMF receptor modelling, Atmos. Chem. Phys., 13, 4375-4392, doi:10.5194/acp-13-4375-2013, 2013a.

Dall'Osto, M., Ovadnevaite, J., Ceburnis, D., Martin, D., Healy, R. M., O'Connor, I. P., Kourtchev, I., Sodeau, J. R., Wenger, J. C., and O'Dowd, C.: Characterization of urban aerosol in Cork city (Ireland) using aerosol mass spectrometry, Atmos. Chem. Phys., 13, 4997-5015, doi:10.5194/acp-13-4997-2013, 2013b.

Day, D. A., Liu, S., Russell, L. M. and Ziemann, P. J. Organonitrate group concentrations in submicron particles with high nitrate and organic fractions in coastal southern California. Atmospheric Environment 44:1970-1979, 2010.

Decesari, S., Allan, J., Plass-Duelmer, C., Williams, B. J., Paglione, M., Facchini, M. C., O'Dowd, C., Harrison, R. M., Gietl, J. K., Coe, H., Giulianelli, L., Gobbi, G. P., Lanconelli, C., Carbone, C., Worsnop, D., Lambe, A. T., Ahern, A. T., Moretti, F., Tagliavini, E., Elste, T., Gilge, S., Zhang, Y., and Dall'Osto, M.: Measurements of the aerosol chemical composition and mixing state in the Po Valley using multiple spectroscopic techniques, Atmos. Chem. Phys., 2014, 14, 12109-12132, doi:10.5194/acp-14-12109-2014.

Drewnick, F., Dall'Osto, M., and Harrison, R. M.: Characterization of aerosol particles from grass mowing by joint deployment of ToF-AMS and ATOFMS instruments, Atmos. Environ., 42, 3006–3017, 2008.

Duce, R.A., La Roche, J., Altieri, K., Arrigo, K.R., Baker, A.R., Capone, D.G., Cornell, S., Dentener, F., Galloway, J., Ganeshram, R.S., Geider, R.J., Jickells, T., Kuypers, M.M., Langlois, R., Liss, P.S., Liu, S.M., Middleburg, J.J., Moore, C.M., Nickovic, S., Oschlies, A., Pedersen, T., Prospero, J., Schlitzer, R., Seitzinger, S., Sorensen, L.L., Uematsu, M., Ulloa, O., Voss, M., Ward, B., Zamora, L.. Impacts of atmospheric anthropogenic nitrogen on the open ocean. Science 320, 893-897, 2008

Fergenson, D. P., Pitesky, M. E., Tobias, H. J., Steele, P. T., Czerwieniec, G. A., Russell, D. H., Lebrilla, C. B., Horn, J. M., Coffee, K. R., Srivastava, A., Pillai, S. P., Shih, M.-T. P., Hall, H. L., Ramponi, A. J., Chang, J. T., Langlois, R. G., Estacio, P. L., Hadley, R. T., Frank, M. and Gard, E. E, Reagentless Detection and Classification of Individual Bioaerosol Particles in Seconds, Anal. Chem., 76, 373-378, 2004.

Furutani, H., J. Jung, K. Miura, A. Takami, S. Kato, Y. Kajii, and M. Uematsu, Single‐particle chemical characterization and source apportionment of iron‐containing atmospheric aerosols in Asian outflow, J. Geophys. Res., 116, D18204, doi:10.1029/2011JD015867, 2011.

Gard, E., Mayer, J. E., Morrical, B. D., Dienes, T., Fergenson ,D. P. and Prather K. A.: Real-time analysis of individual atmospheric aerosol particles: Design and performance of a portable ATOFMS, Anal. Chem., 69, 4083-4091, 1997.

Gard, E. E., M. J. Kleeman, D. S. Gross, L. S. Hughes, J. O. Allen, B. D. Morrical, D. P. Fergenson, T. Dienes, M. E. Galli, R. J. Johnson, G. R. Cass, and K. A. Prather, Direct observation of heterogeneous chemistry in the atmosphere, Science, 279, 1184–1187, 1998.

Ge, X., Wexler, A. S., and Clegg, S. L.: Atmospheric amines – Part I. A review, Atmos. Environ., 45, 524–546, doi:10.1016/j.atmosenv.2010.10.012, 2011.

Giorio, C., Tapparo, M., Dall'Osto, M., Harrison, Roy M., Beddows, D.C.S, Di Marco, C., Nemitz, E. Comparison of three techniques for analysis of data from an Aerosol Time-of-Flight Mass Spectrometer, Atmospheric Environment, Volume 61, Pages 316-326, 2012

Goldstein, A. H. and Galbally, I. E.: Known and unexplored organic constituents in the earth's atmosphere, Environ. Sci.Technol., 41, 1514-1521, 2007.

Gross, D. S., Galli, M. E., Silva, P. J., and Prather, K. A. Relative Sensitivity Factors for Alkali Metal and Ammonium Cations in Single Particle Aerosol Time-of-flight Mass Spectra, Anal. Chem., 72, 416–422, 2000.

Guazzotti, S.A., Suess, D.T., Coffee, K.R., Quinn, P.K., Bates, T.S., Wisthaler, A., Hansel, A., Ball, W.P., Dickerson, R.R., Neususs, C., Crutzen, P.J., Prather, K.A.. Characterization of carbonaceous aerosols outflow from India and Arabia: biomass/biofuel burning and fossil fuel combustion. Journal of Geophysical Research—Atmospheres 108 (D15) (Article no. 4485), 2003.

Hanson, D. R., McMurry, P. H., Jiang, J. K., Huey, G., and Tanner, D.: Ambient Pressure Proton Transfer mass spectrometry: detection of ammonia and amines, Environ. Sci. Technol., 45, 8881–8888, 2011.

Harrison, R. M., Dall'Osto, M., Beddows, D. C. S., Thorpe, A. J., Bloss, W. J., Allan, J. D., Coe, H., Dorsey, J. R., Gallagher, M., Martin, C., Whitehead, J., Williams, P. I., Jones, R. L., Langridge, J. M., Benton, A. K., Ball, S. M., Langford, B., Hewitt, C. N., Davison, B., Martin, D., Petersson, K. F., Henshaw, S. J., White, I. R., Shallcross, D. E., Barlow, J. F., Dunbar, T., Davies, F., Nemitz, E., Phillips, G. J., Helfter, C., Di Marco, C. F., and Smith, S.: Atmospheric chemistry and physics in the atmosphere of a developed megacity (London): an overview of the REPARTEE experiment and its conclusions, Atmos. Chem. Phys., 12, 3065-3114, doi:10.5194/acp-12-3065-2012, 2012.

Healy, R. M., O'Connor, I. P., Hellebust, S., Allanic, A., Sodeau, J. R., and Wenger, J. C.: Characterisation of single particles from in-port ship emissions, Atmos. Environ., 43, 6408–6414, 2009.

Healy, R. M., Sciare, J., Poulain, L., Crippa, M., Wiedensohler, A., Prévôt, A. S. H., Baltensperger, U., Sarda-Estève, R., McGuire, M. L., Jeong, C.-H., McGillicuddy, E., O'Connor, I. P., Sodeau, J. R., Evans, G. J., and Wenger, J. C.: Quantitative determination of carbonaceous particle mixing state in Paris using single-particle mass spectrometer and aerosol mass spectrometer measurements, Atmos. Chem. Phys., 13, 9479-9496, doi:10.5194/acp-13-9479-2013, 2013

Healy, R. M., Riemer, N., Wenger, J. C., Murphy, M., West, M., Poulain, L., Wiedensohler, A., O'Connor, I. P., McGillicuddy, E., Sodeau, J. R., and Evans, G. J.: Single particle diversity and mixing state measurements, Atmos. Chem. Phys., 14, 6289-6299, doi:10.5194/acp-14-6289-2014, 2014.

Healy RM, Evans GJ, Murphy M, Sierau B, Arndt J, McGillicuddy E, O'Connor IP, Sodeau JR, Wenger JC. Single-particle speciation of alkylamines in ambient aerosol at five European sites. Anal Bioanal Chem. Aug;407(20):5899-909. doi: 10.1007/s00216-014-8092-1, 2015.

Hodzic A, Wiedinmyer C, Salcedo D, Jimenez JL. Impact of trash burning on air quality in Mexico City. Environ Sci Technol, 1;46(9):4950-7, 2012

Jeong, C.-H., McGuire, M. L., Godri, K. J., Slowik, J. G., Rehbein, P. J. G., and Evans, G. J.: Quantification of aerosol chemical composition using continuous single particle measurements, Atmos. Chem. Phys., 11, 7027-7044, doi:10.5194/acp-11-7027-2011, 2011

Jimenez, J. L., Canagaratna, M. R., Donahue, N. M., Prevot, A. S. H., Zhang, Q., Kroll, J. H., DeCarlo, P. F., Allan, J. D., Coe, H., Ng, N. L., Aiken, A. C., Docherty, K. S., Ulbrich, I. M., Grieshop, A. P., Robinson, A. L., Duplissy, J., Smith, J. D., Wilson, K. R., Lanz, V. A., Hueglin, C., Sun, Y. L., Tian, J., Laaksonen, A., Raatikainen, T., Rautiainen, J., Vaattovaara, P., Ehn, M., Kulmala, M., Tomlinson, J. M., Collins, D. R., Cubison, M.J., Dunlea, E. J., Huffman, J. A., Onasch, T. B., Alfarra, M. R., Williams, P. I., Bower, K., Kondo, Y., Schneider, J., Drewnick, F., Borrmann, S., Weimer, S., Demerjian, K., Salcedo, D., Cottrell, L., Griffin, R., Takami, A., Miyoshi, T., Hatakeyama, S., Shimono, A., Sun, J. Y., Zhang, Y. M., Dzepina, K., Kimmel, J. R., Sueper, D., Jayne, J. T., Herndon, S. C., Trimborn, A. M.,Williams, L. R., Wood, E. C., Middlebrook, A. M., Kolb, C.E., Baltensperger, U., and Worsnop, D. R.: Evolution of organic aerosols in the atmosphere, Science, 326, 1525–1529, 2009.

Jordi, A., Basterretxea, G., Tovar-Sánchez, A., Alastuey, A., Xavier Querol X. Copper aerosols inhibit phytoplankton growth in the Mediterranean Sea PNAS 2012 ; published ahead of print December 10, 2012, doi:10.1073/pnas.1207567, 2012

Kellogg, C. A. and Griffin, D.W., Aerobiology and the global transport of desert dust, Trends Ecol Evol, 21, 638–644, doi: 10.1016/j.tree.2006.07.004, 2006.

Laskin, A., Laskin, J., and Nizkorodov, S. A.: Mass spectrometric approaches for chemical characterization of atmospheric aerosols: critical review of the most recent advances, Environ. Chem., 9, 163–189, 2012

McLafferty, F. W.: Interpretation of Mass Spectra, 3rd Edn., p. 303, 1993.

Mc Murry P.H. A review of atmospheric aerosol measurementsq Atmos, Environ 34:1959–1999, 2000

Mohr, C., DeCarlo, P. F., Heringa, M. F., Chirico, R., Slowik, J. G., Richter, R., Reche, C., Alastuey, A., Querol, X., Seco, R., Penuelas, J., Jimenez, J. L., Crippa, M., Zimmermann, R., Baltensperger, U., and Prevot, A. S. H.: Identification and quantification of organic aerosol from cooking and other sources in Barcelona using aerosol mass spectrometer data, Atmos. Chem. Phys., 12, 1649–1665, doi:10.5194/acp-12-1649-2012, 2012

Moffet, R. C., de Foy, B., Molina, L. T., Molina, M. J., and Prather, K. A.: Measurement of ambient aerosols in northern Mexico City by single particle mass spectrometry, Atmos. Chem. Phys., 8, 4499-4516, doi:10.5194/acp-8-4499-2008, 2008

Moffet, R. C. and Prather, K. A.: In-situ measurements of the mixing state and optical properties of soot with implications for radiative forcing estimates, Proc. Natl. Acad. Sci. U. S. A., 106, 11872–11877, 2009.

Moffet, R. C., H. Furutani, T. C. Rödel, T. R. Henn, P. O. Sprau, A. Laskin, M. Uematsu, and M. K. Gilles, Iron speciation and mixing in single aerosol particles from the Asian continental outflow, J. Geophys. Res., 117, D07204, doi:10.1029/2011JD016746, 2012

Murphy, S. M., Sorooshian, A., Kroll, J. H., Ng, N. L., Chhabra, P., Tong, C., Surratt, J. D., Knipping, E., Flagan, R. C., and Seinfeld, J. H.: Secondary aerosol formation from atmospheric reactions of aliphatic amines, Atmos. Chem. Phys., 7, 2313-2337, doi:10.5194/acp-7-2313-2007, 2007

Neubauer, K. R., Johnston, M. V., and Wexler, A. S.: Humidity effects on the mass spectra of single aerosol particles, Atmos. Environ., 32, 2521–2529, 1998.

O'Brien R.E., A. Laskin, J. Laskin, S. Liu, R. Weber, L. Russell, and A.H. Goldstein. Molecular Characterization of Organic Aerosol Using Nanospray Desorption/Electrospray Ionization Mass Spectrometry: CalNex 2010 field study. Atmospheric Environment 68:265-272. doi:10.1016/j.atmosenv.2012.11.056, 2013

Pastor, S.H., J.O. Allen, L.S. Hughes, P. Bhave, G.R. Cass, and K.A. Prather, Ambient single particle analysis in Riverside, California by aerosol time-of-flight mass spectrometry during the SCOS97-NARSTO, Atmospheric Environment, 37, S239-S258, 2003.

Pattanaik, S.; Huggins, F. E.; Huffman, G. P.; Linak, W. P.; Miller, C. A. XAFS studies of nickel and sulfur speciation in residual oil fly-ash particulate matters (ROFA PM). Environ. Sci. Technol. 41 (4), 1104–1110, 2007.

Pratt, K. A., Hatch, L. E., and Prather, K. A.: Seasonal volatility dependence of ambient particle phase amines, Environ. Sci. Technol., 43, 5276–5281, 2009.

Pratt, K. A. and Prather, K. A.: Mass spectrometry of atmospheric aerosols – Recent developments and applications, Part II: On-line mass spectrometry techniques, Mass Spectrom. Rev., 31, 17–48, 2012

Prospero, J., Blades, E., Mathison, G., and Naidu, R.: Interhemispheric transport of viable fungi and bacteria from Africa to the Caribbean with soil dust, Aerobiologia, 21, 1–19, 2005.

Qin, X. Y., Bhave, P. V., and Prather, K. A.: Comparison of two methods for obtaining quantitative mass concentrations from aerosol time-of-flight mass spectrometry measurements, Anal. Chem., 78, 6169–6178, 2006.

Rebotier, T. P. and Prather, K. A.: Aerosol time-of-flight mass spectrometry data analysis: A benchmark of clustering algorithms, Anal. Chim. Acta, 585, 38–54, 2007.

Reche, C., Querol, X., Alastuey, A., Viana, M., Pey, J., Moreno, T., Rodríguez, S., González, Y., Fernández-Camacho, R., de la Rosa, J., Dall'Osto, M., Prévôt, A. S. H., Hueglin, C., Harrison, R. M., and Quincey, P.: New considerations for PM, Black Carbon and particle number concentration for air quality monitoring across different European cities, Atmos. Chem. Phys., 11, 6207-6227, doi:10.5194/acp-11-6207-2011, 2011

Reche, C., Viana, M., Pandolfi, M., Alastuey, A., Moreno, T., Amato, F., Ripoll, A., and Querol, X.: Urban NH3 levels and sources in a Mediterranean environment, Atmos. Environ., 57, 153–164, 2012.

Rehbein, P. J. G., Jeong, C.-H. , McGuire M. L., Yao X., Corbin J. C., Evans G. J., Cloud and fog processing enhanced gas-to-particle partitioning of trimethylamine. Environ. Sci. Technol., 45, 4346. doi:10.1021/ES1042113, 2011

Reilly, P. T. A.; Lazar, A. C.; Gieray, R. A.; Whitten, W. B.; Ramsey, J. M. The elucidation of charge-transfer-induced matrix effects in environmental aerosols via real-time aerosol mass spectral analysis of individual airborne particles. Aerosol Sci. Technol., 33, 135-152, 2000.

Reinard, M.S., Johnston, M.V., Ion formation mechanism in laser desorption ionization of individual particles. Journal of the American Society for Mass Spectrometry 19, 389e399, 2008

Salcedo, D., Onasch, T. B., Aiken, A. C., Williams, L. R., de Foy, B., Cubison, M. J., Worsnop, D. R., Molina, L. T., and Jimenez, J. L.: Determination of particulate lead using aerosol mass spectrometry: MILAGRO/MCMA-2006 observations, Atmos. Chem. Phys., 10, 5371-5389, doi:10.5194/acp-10-5371-2010, 2010

Schoolcraft, T. A.; Constable, G. S.; Jackson, B.; Zhigilei, L. V.; Garrison, B. J. Molecular dynamics simulations of laser disintegration of amorphous aerosol particles with spatially non- uniform absorption. Nucl. Instrum. Methods Phys. Res., Sect. B, 180, 245-250, 2001.

Schofield, M.J., 2004. Sources and properties of airborne particulate matter. Ph.D. Thesis. School of Geography, Earth and Environmental Sciences. Birmingham, University of Birmingham.

Silva, P. J., Liu, D.-Y., Noble, C. A., and Prather, K. A.: Size and chemical characterization of individual particles resulting from biomass burning of local Southern California species, Environ. Sci. Technol., 33, 3068–3076, 1999.

Silva, P. J. and Prather K. A.: Interpretation of mass spectra from organic compounds in aerosol time-of-flight mass spectrometry, Anal. Chem., 72, 3553-3562, 2000.

Silva, P. J.; Erupe, M. E.; Price, D.; Elias, J.; Malloy, Q. G. J.; Li, Q.; Warren, B.; Cocker, D. R. Trimethylamine as precursor to secondary organic aerosol formation via nitrate radical reaction in the atmosphere. Environ. Sci. Technol, 42 (13), 4689–4696, 2008.

Shiraiwa, M., Kondo, Y., Moteki, N., Takegawa, N., Miyazaki, Y.,and Blake, D. R.: Evolution of mixing state of black carbonin polluted air from Tokyo, Geophys. Res. Lett., 34, L16803,doi:10.1029/2007GL029819, 2007.

Sleiman, M., Destaillats, H., Smith, J., Liu, C.L., Ahmed, M., Wilson, K.R., Gundel, L.A. Secondary organic aerosol formation from ozone-initiated reactions with nicotine and secondhand smoke. Atmospheric Environment 44, 4191-4198, 2010.

Solazzo, E., Cai, X., and Vardoulakis, S.: Modelling wind flow and vehicle-induced turbulence in urban streets, Atmos. Environ., 42, 4918–4931, 2008.

Song, X. H., Hopke, P. K., Fergenson, D. P., and Prather, K. A.: Classification of single particles analyzed by ATOFMS using an artificial neural network, ART-2A, Anal. Chem., 71, 860–865, 1999

Spencer, M. T., Shields, L. G., Sodeman, D. A., Toner, S. M.and Prather K. A.: Comparison of oil and fuel particle chemical signatures with particle emissions from heavy and light duty vehicles, Atmos. Environ., 40, 5224-5235, 2006.

Su, Y. X., Sipin, M. F., Furutani, H., and Prather, K. A. Development and Characterization of an Aerosol Time-of-Flight Mass Spectrometer with Increased Detection Efficiency. Anal. Chem., 76(3):712–719, 2004.

Sureda, X., Martinez-Sanchez, J.M., Lopez, M.J., Fu, M., Aguero, F., Salto, E., Nebot, M.; Fernandez, E; Secondhand smoke levels in public building main entrances: outdoor and indoor PM2.5 assessment, Tobacco Control 21:543–548, 2012.

Volkamer, R., Jimenez, J. L., San Martini, F., Dzepina, K., Zhang, Q., Salcedo, D., Molina, L. T., Worsnop, D. R. and Molina, M. J. Secondary organic aerosol formation from anthropogenic air pollution: Rapid and higher than expected, Geophysical Research Letters, 33, L17811, doi:10.1029/2006GL026899, 2006.

Wayne, R. P., Barnes, I., Biggs, P., Burrows, J. P., Canasa-Mas, C. E., Hjorth, J., Le Bras, G., Moorgat, G. K., Perner, D., Poulet, G., Restelli, G., and Sidebottom, H.: The nitrate radical physics, chemistry, and the atmosphere., Atmos. Environ., 25A, 1–203, 1991.

WHO: Health Aspects of Air pollution, Syst.Rew.of health asp. of air poll. in Europe, Copenhagen, 2004

WHO http://www.who.int/whosis/whostat/EN_WHS10_Full.pdf). Last access December 2012

Atmos. Chem. Phys. Discuss., doi:10.5194/acp-2015-986, 2016
Manuscript under review for journal Atmos. Chem. Phys.
Published: 5 February 2016

Atmospheric Chemistry and Physics Discussions

Monitoring RS site	Particle type	particle number	%	Monitoring UB site	Particle type	particle number	%
Local & Regional EC	*EC_Aged_L*	277,151	31.1	Local & Regional EC	*EC_Aged_L*	52,074	23.8
	EC_Aged_R	202,227	22.7		*EC_Aged_R*	76,678	35.1
Secondary inorganic	*LRT-NIT*	102,909	11.6	Secondary inorganic	*LRT-NIT*	9,982	4.6
	Loc-NIT	37,790	4.2		*Loc-NIT*	15,931	7.3
	LRT-SUL	52,420	5.9		*LRT-SUL*	6,635	3.0
Sea Salt	*NaCl-NIT*	75,204	8.4	Sea Salt	*NaCl-NIT*	8,166	3.7
	NaCl	8,926	1.0		*NaCl*	31,853	14.6
Industry	*Fe*	7,201	0.8	Industry	*Fe*	5,564	2.5
	Pb	577	0.1		*Pb*	382	0.2
Combustion	*K-CN*	21,515	2.4	Combustion	*K-CN*	2,778	1.3
Monitoring RS site	**Particle type**	**particle number**	**%**	**Monitoring UB site**	**Particle type**	**particle number**	**%**
RS particles	*Amine (POA 58)*	6,698	0.8	UB particles	*Soil-Saharan*	2,842	1.3
	Amine (SOA 114)	3,672	0.4		*Soil-Ca*	2,482	0.9
	Amine (SOA 59)	2,141	0.2		*Oil-V*	1,875	0.9
	Amine (EST 84)	4,888	0.5		*Veg-KP*	3,897	1.7
	Org. (Lub Oil)	16,273	1.8				
	Org.(OC-CHO)	42,680	4.8				
	Org. (Aro-NIT)	15,306	1.7				
	Org. (OC-NIT)	13,295	1.5				
TOTAL RS		**890,873**	**100**	**TOTAL UB**		**221,139**	**100**

Table 1 ATOFMS particle clusters identified from the SAPUSS campaign.

Atmos. Chem. Phys. Discuss., doi:10.5194/acp-2015-986, 2016
Manuscript under review for journal Atmos. Chem. Phys.
Published: 5 February 2016

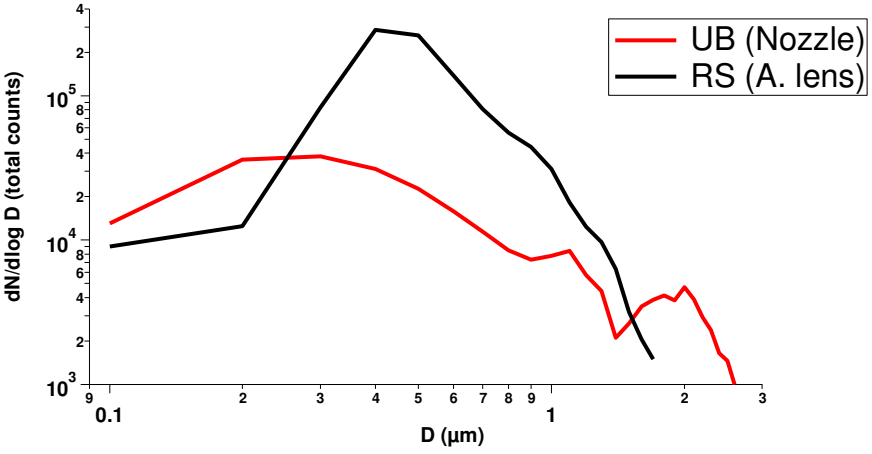

Figure 1. Size distributions of collected ATOFMS particles at the two SAPUSS monitoring sites

Atmos. Chem. Phys. Discuss., doi:10.5194/acp-2015-986, 2016
Manuscript under review for journal Atmos. Chem. Phys.
Published: 5 February 2016

Atmospheric Chemistry and Physics Discussions

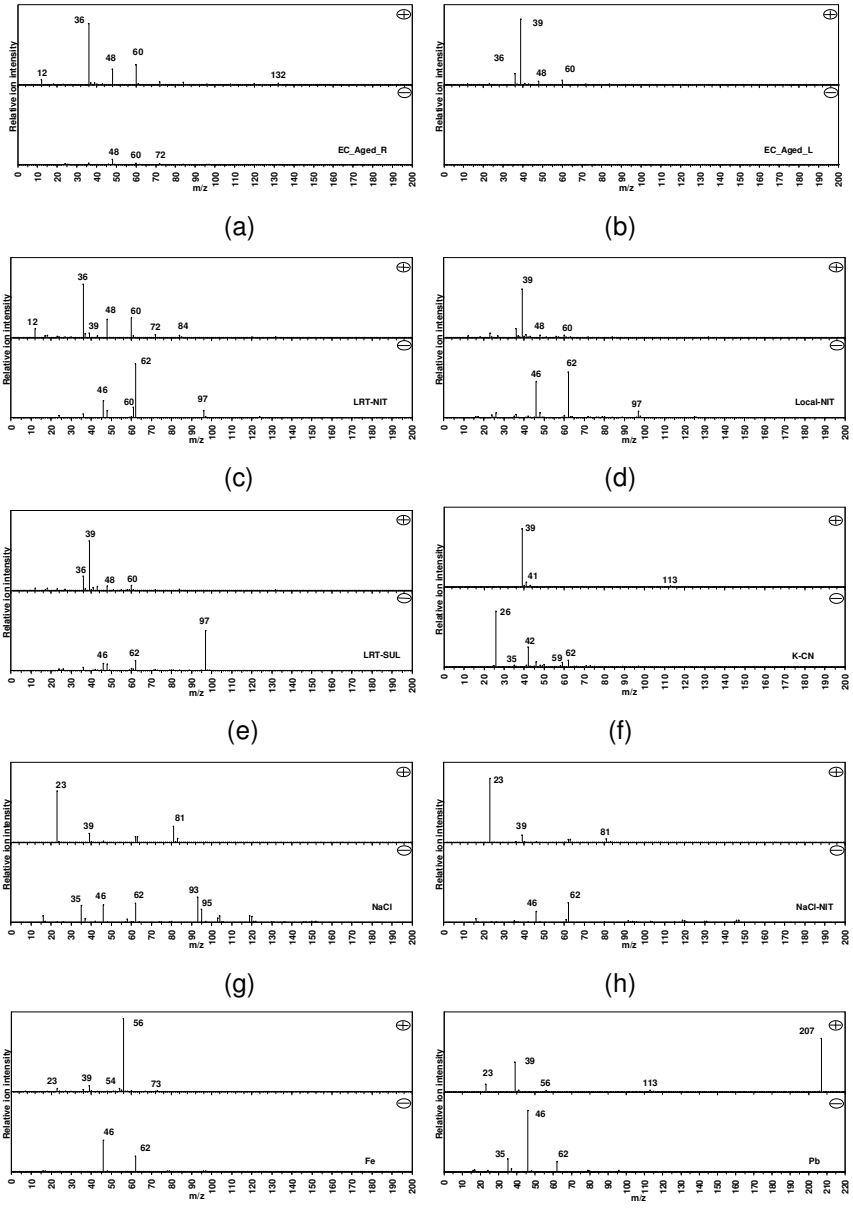

Figure 2. Average mass spectra of the 10 single particle types observed at both the RS and UB sites.

Atmos. Chem. Phys. Discuss., doi:10.5194/acp-2015-986, 2016
Manuscript under review for journal Atmos. Chem. Phys.
Published: 5 February 2016

Atmospheric Chemistry and Physics Discussions

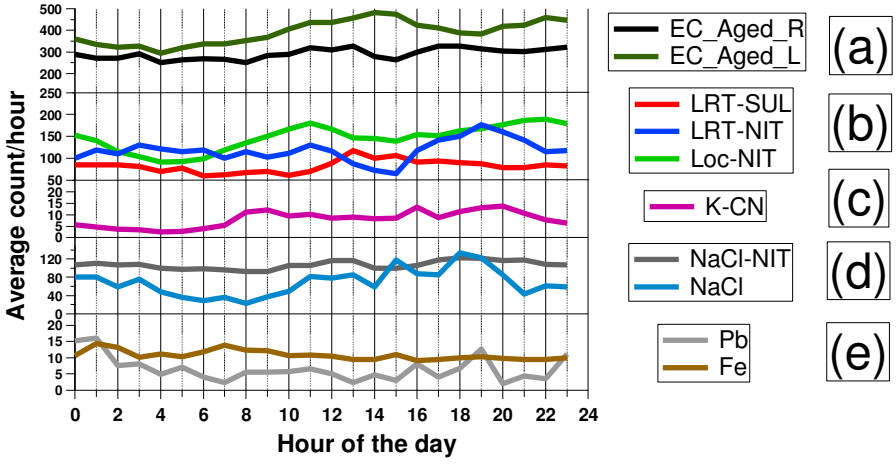

Figure 3. Diurnal profiles of the common particle types detected at both the RS and UB sites. Differences between RS and UB sites were minor and average diurnal profiles are presented.

Atmos. Chem. Phys. Discuss., doi:10.5194/acp-2015-986, 2016
Manuscript under review for journal Atmos. Chem. Phys.
Published: 5 February 2016

Atmospheric Chemistry and Physics Discussions

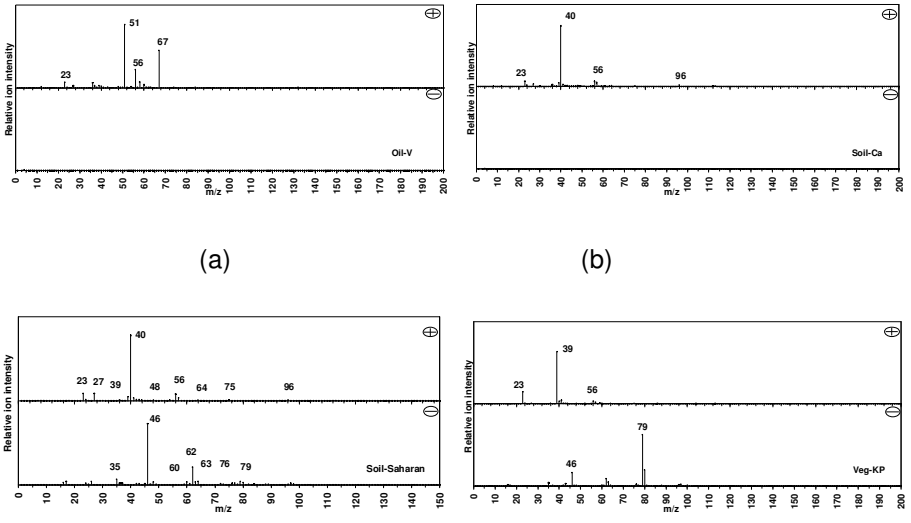

Figure 4. Average mass spectra of the 4 single particle types only observed at the UB site.

Atmos. Chem. Phys. Discuss., doi:10.5194/acp-2015-986, 2016
Manuscript under review for journal Atmos. Chem. Phys.
Published: 5 February 2016

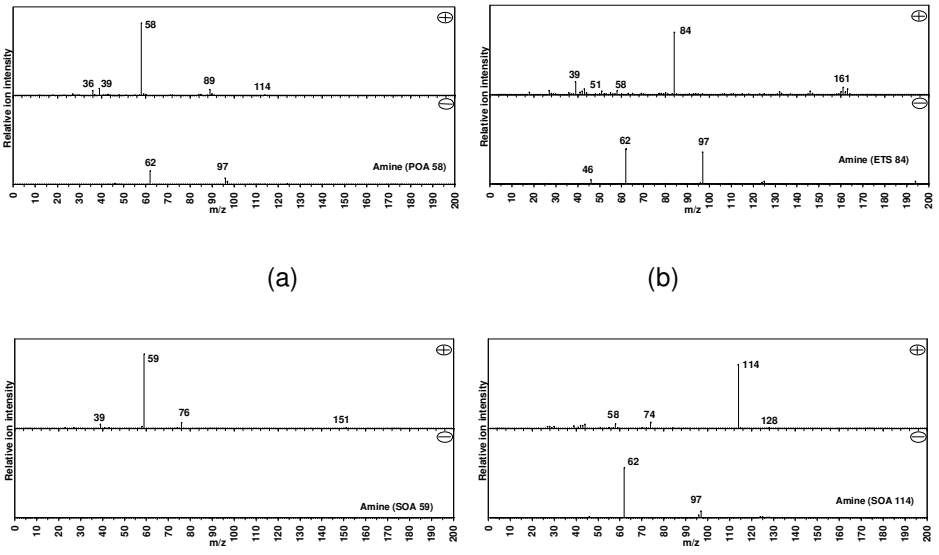

Figure 5. Average mass spectra of the 4 amine-containing single particle types only observed at the RS site.

Atmos. Chem. Phys. Discuss., doi:10.5194/acp-2015-986, 2016
Manuscript under review for journal Atmos. Chem. Phys.
Published: 5 February 2016

Atmospheric Chemistry and Physics Discussions

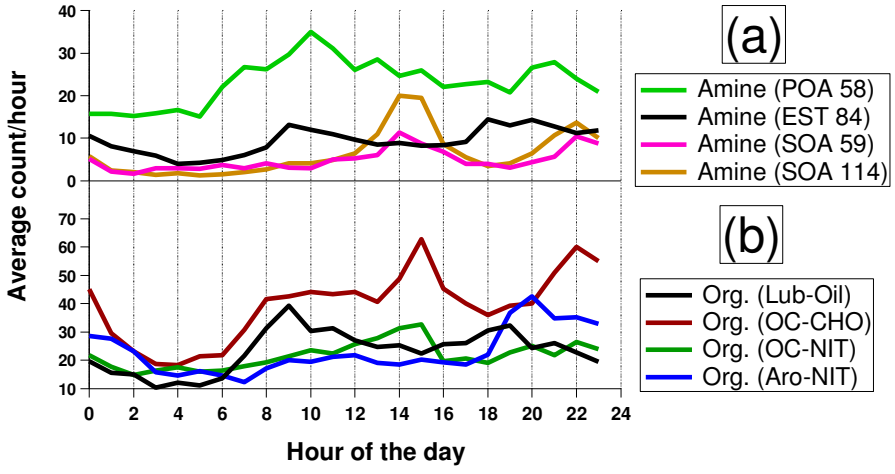

Figure 6. Diurnal trend of Amines (a) and organic-rich (b) particle types detected at the RS site. . Differences between RS and UB sites were minor and average diurnal profiles are presented.

Atmos. Chem. Phys. Discuss., doi:10.5194/acp-2015-986, 2016
Manuscript under review for journal Atmos. Chem. Phys.
Published: 5 February 2016

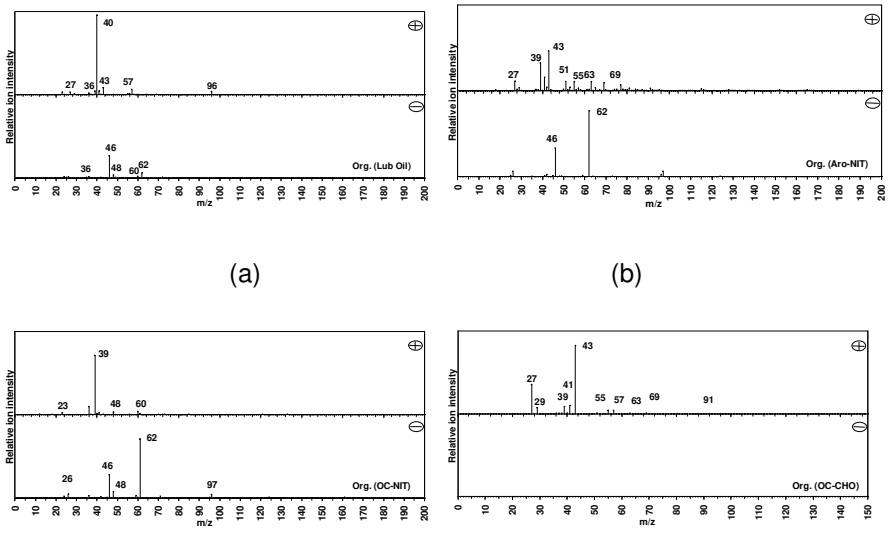

Figure 7. Average mass spectra of the 4 OC-rich single particle types only observed at the RS site.